

This is a repository copy of *Effect of Loading on Field Uniformity:Energy Diffusion in Reverberant Environments*.

White Rose Research Online URL for this paper:

<https://eprints.whiterose.ac.uk/114564/>

Version: Accepted Version

Proceedings Paper:

Robinson, M. P. orcid.org/0000-0003-1767-5541, Flintoft, I. D. orcid.org/0000-0003-3153-8447, Dawson, J. F. orcid.org/0000-0003-4537-9977 et al. (4 more authors) (2017) Effect of Loading on Field Uniformity:Energy Diffusion in Reverberant Environments. In: 32nd URSI General Assembly and Scientific Symposium (URSI GASS). , Montreal

Reuse

This article is distributed under the terms of the Creative Commons Attribution-NonCommercial-NoDerivs (CC BY-NC-ND) licence. This licence only allows you to download this work and share it with others as long as you credit the authors, but you can't change the article in any way or use it commercially. More information and the full terms of the licence here: <https://creativecommons.org/licenses/>

Takedown

If you consider content in White Rose Research Online to be in breach of UK law, please notify us by emailing eprints@whiterose.ac.uk including the URL of the record and the reason for the withdrawal request.



Effect of Loading on Field Uniformity: Energy Diffusion in Reverberant Environments

M. P. Robinson⁽¹⁾, I. D. Flintoft⁽¹⁾, J. F. Dawson⁽¹⁾, A. C. Marvin⁽¹⁾, F. I. Funn⁽²⁾, L. Dawson⁽¹⁾ and X. Zhang⁽¹⁾

(1) University of York, York, YO10 5DD, UK, <http://www.york.ac.uk>

(2) Republic of Singapore Airforce

Abstract

In reverberant electromagnetic environments such as reverberation chambers, shielding enclosures, vehicles and buildings, the electromagnetic energy density is often assumed to be uniform and the direction of arrival of electromagnetic waves (Poynting vector) and their polarisation is assumed uniformly distributed. This is the basis of the power balance method for electromagnetic coupling analysis and much of the theory of reverberation chambers. However significant field inhomogeneity is often encountered in practice when significant losses are present. In this paper we show why this must be so when an energy flow exists from the source of energy to absorptive elements, and how the non-uniformity can be determined using a diffusion based solution. The diffusion based solution, though not as computationally efficient as the power balance method, is still much more efficient than a full-wave approach.

1. Introduction

The theory of reverberation chambers (RCs) was developed on the assumption that “the electromagnetic field is a superposition of quasi-plane waves having random amplitudes, directions, polarizations and phases” [1]. This was given a more detailed mathematical foundation by Hill [2] and extended to the more general case of electromagnetic power balance (PWB) in enclosures with apertures in [3] and [4].

The PWB formulation assumes that the electromagnetic energy in a cavity is completely diffuse due to the large number of reflections from the cavity walls and any internal structure. This means that the average energy flow of the ensemble of waves is the same in every direction. In practice, an energy source is present in one location, whilst energy absorption occurs at other locations in the chamber. There must be a net flow of energy between the sources and absorbers of energy. This implies that the field cannot be completely uniform.

When the losses in a cavity are small the frequent reflections from walls and contents act to keep the energy density uniform, but in the case of moderate losses the assumption of uniform energy density becomes inaccurate. This effect has also been observed for the acoustic reverberation problem [5]. In our recent paper [6] we evaluated the diffusion approach for electromagnetic problems. Here, we provide a simplified overview of the

method and results presented in [6], which demonstrates the efficacy of the diffusion method.

2. The Diffusion Model

The energy density due to the electromagnetic fields in a reverberant environment can be written as:

$$W(\mathbf{r}) = \frac{1}{2}(\epsilon_0\langle|\mathbf{E}(\mathbf{r})|^2\rangle + \mu_0\langle|\mathbf{H}(\mathbf{r})|^2\rangle) \quad (1)$$

where $|\mathbf{E}(\mathbf{r})|^2$ and $|\mathbf{H}(\mathbf{r})|^2$ are the sums of the squares of the magnitudes of the rms values of the three orthogonal field components. The angle brackets $\langle\cdot\rangle$ represent an average over a statistical ensemble of systems. The position in space is denoted by the vector \mathbf{r} . The energy in the each of the electric and magnetic field components is often assumed to be equal. This is true in the volume of a cavity well clear of any conductor, however it is not necessarily always the case: e.g. at the conducting wall of a cavity the tangential electric field components go to zero whilst the tangential magnetic fields increase in value even if the energy density remains constant [7]. It should therefore be noted that in this paper when we present energy density, it does not imply that it is distributed equally across all field components.

By replacing the assumption of constant power density, used in power balance models, with a model where, in the steady state, the energy in a cavity satisfies the diffusion equation:

$$(D\nabla^2 + A_V)W(\mathbf{r}, t) = P^{\text{TRP}}\delta^{(3)}(\mathbf{r} - \mathbf{r}_s) \quad (2)$$

where D is the diffusivity, A_V is a volumetric energy loss rate, $\delta^{(3)}$ is the 3-dimensional delta function, and we have assumed that there is an isotropic point source of total radiated power P^{TRP} located at \mathbf{r}_s . The diffusivity depends on the mean free path (\bar{l}) between scattering of rays in the cavity:

$$D = \bar{l}c_0/3 \quad (3)$$

Where c_0 is the propagation velocity of the electromagnetic waves in the cavity. Considering only the scattering from the cavity walls, the mean free path would be:

$$\bar{l}_{\text{wall}} = 4V/S_V \quad (4)$$

where V is the volume of the cavity and S_V is the surface area of the cavity walls which are assumed to be highly reflective. Similarly other scattering objects affect the

mean free path so that the overall mean free path is the harmonic mean of the paths due to the walls and objects:

$$\bar{l}^{-1} = \bar{l}_{\text{wall}}^{-1} + \bar{l}_{\text{con}}^{-1}. \quad (5)$$

where the mean free path due to the scattering objects is:

$$\bar{l}_{\text{con}} = 4V/S_{\text{con}} \quad (6)$$

and S_{con} is their surface area.

Energy absorbed by the cavity walls and other objects and can be represented by a boundary condition:

$$\left(D\hat{\mathbf{n}} \cdot \nabla + c_0 \Sigma_{\alpha}^a(\mathbf{r}) \right) W(\mathbf{r}) = 0 \quad (7)$$

where $\hat{\mathbf{n}}$ is an outward unit normal vector and $\Sigma_{\alpha}^a(\mathbf{r})$ is an absorption factor related to the average reflection coefficient of the object:

$$\Sigma_{\alpha}^a(\mathbf{r}) = \alpha^a(\mathbf{r})/4, \quad (8)$$

where $\alpha^a(\mathbf{r})$ is the average absorption efficiency of the object.

Cavities coupled via apertures can be described directly by the model of the previous section if the field in the aperture can be assumed to be diffuse. If the energy density is assumed constant the diffusion model reduces to the power balance formulation of Hill [2].

3. Simple Test Case

We investigated the method in a cavity with a removable partition and cylindrical absorber. Both partition and absorber span the full height of the cavity so that the problem can be simplified to a two dimensional one. This is shown in Figure 1, where the small black dots represent the field measurement locations in the $z = h$ plane. The location of the source antenna is also shown. The enclosure was fabricated from brass with a removable lid. Dimensions are given in Table 1.

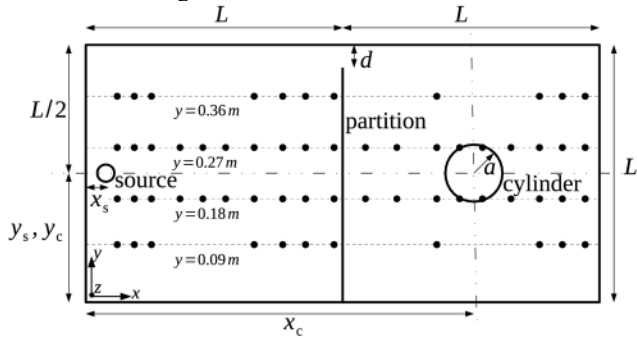


Figure 1. Cross-section of the cuboid enclosure used for the canonical examples and validation measurements.

4. Measurement Methodology

The mismatch corrected insertion gain, IG , between the source and measurement probe antennas was determined from the scattering parameters measured using a vector network analyzer at 1600 equi-spaced frequency points in the band 8-8.5 GHz.

Table 1. Parameters for the Test Cases

Parameter	Value	Parameter	Value
L	0.45 m	x_s	0.01 m
h	0.45 m	y_s	0.225 m
d	0.04 m	z_s	0.225 m
a	0.05 m	P^t	1 W
α_{wall}^a	0.0027	x_c (Cs. A)	0.7 m
α_c^a	0.95	x_c (Cs. B)	0.675 m
		y_c	0.225 m

$$IG = |S_{21}|^2 / (1 - |S_{11}|^2)(1 - |S_{22}|^2) \quad (9)$$

The diffuse field power density in the cavity was then estimated by averaging the insertion gain over the frequency band:

$$S = c_0 w = 8\pi \langle IG \rangle / \lambda^2 \quad (10)$$

where λ is wavelength. The mode density in the cavity was about 10 MHz^{-1} at 8 GHz and the measured mode bandwidth was about 9 MHz when loaded, suggesting that about 50 independent samples of the field are included in the frequency average. Accordingly, the 1-sigma confidence interval on the measured average powers is about 1.3 dB [9].



Figure 2. Measurement of the absorbing cylinder ACS in a reverberation chamber

The Q-factor of the empty cavity was $\sim 25,000$ based on the insertion gain measurement, and the absorption efficiency, α_{wall}^a , of the cavity walls (Table 1) was determined by fitting this using the PWB model.

The average absorption cross-section, σ_{cyl}^a , of the absorbing cylinder, with metal caps placed on either end, was measured in a reverberation chamber (Figure 2) using the methodology described in [10]. The absorption efficiency (Table 1) was then computed as:

$$\alpha_{\text{cyl}}^a = 4 \sigma_{\text{cyl}}^a / 2\pi a h \quad (11)$$

It should be noted that the cylinder is in its resonant scattering region in the vicinity of 8.5 GHz where the results below are presented, so it has a larger absorption

than would be expected from the manufacturer's plane-wave data for the absorber material.

5. Diffusion model v PWB and measurements

For an initial evaluation we modelled the test case with a two dimensional approximation, using the open-source solver FreeFEM++ [8]. The details of the conversion to a 2-dimensional problem are given in [6]. We considered the box both with (Case A) and without (Case B) the partition. The dimensions of the problem and absorption efficiencies of the walls are given in Table 1.

5.1. Enclosure with no partition

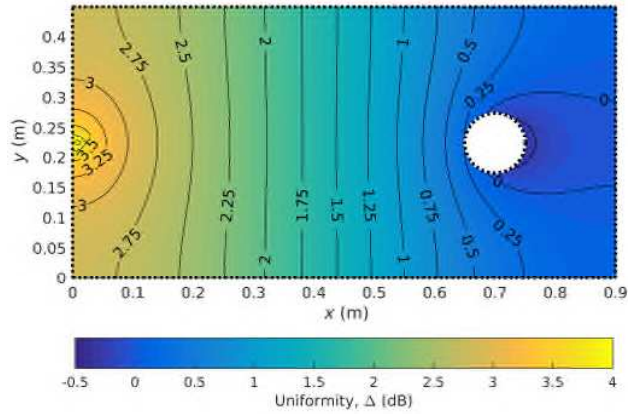


Figure 3. The diffuse energy density uniformity for enclosure with absorbing cylinder.

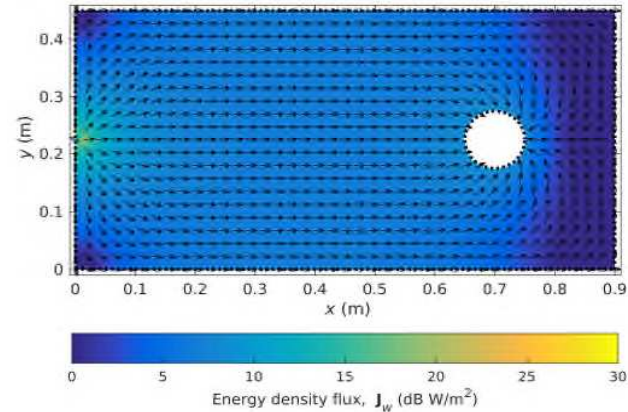


Figure 4. Diffuse energy density flux, $J_w(x, y, h/2)$, in the cuboid enclosure with an absorbing cylinder with $\alpha_c^a = 1.0$.

Figure 3 shows the ratio of energy density obtained with no partition using the diffusion model, compared to the case predicted by a PWB model with the same parameters. It can be seen that the diffusion model shows an increased energy density at the source and a reduced energy density near the absorber. Note that the energy density near the walls is reduced a little due to the small absorption in the walls. As might be expected a net energy flow (Figure 4) can be seen from the source to the absorbing cylinder. With no absorbing cylinder present, the diffusion result was identical to that of the power balance model.

Figure 5 compares the results from the energy diffusion model (EDM), the power balance solution and measurements using small probe antennas on the wall of the enclosure along a line in the x -direction. It can be seen that in the case with no loading cylinder the measurement, PWB and diffusion results are almost identical. For the case where the cavity is loaded with the absorbing cylinder, the diffusion and measured results show similar trends but differ somewhat in absolute value. We believe this to be due to the difficulty of accurately calibrating the measurements and statistical variation as only frequency stirring was used. The PWB solution for the loaded case is constant as expected.

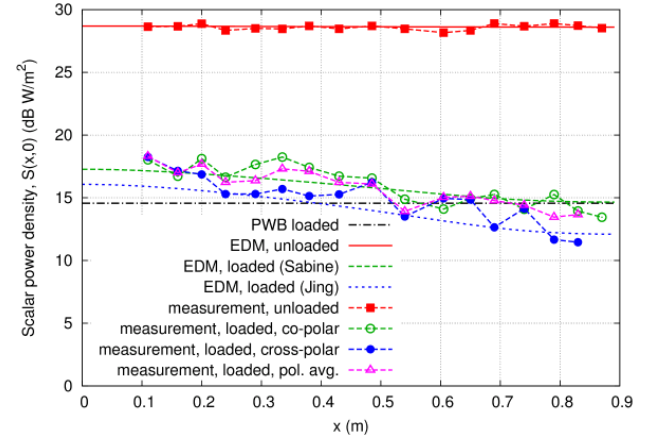


Figure 5. Comparing the PWB, diffusion and measured results along the $y = 0$ wall at half the height of the enclosure at 8.5 GHz.

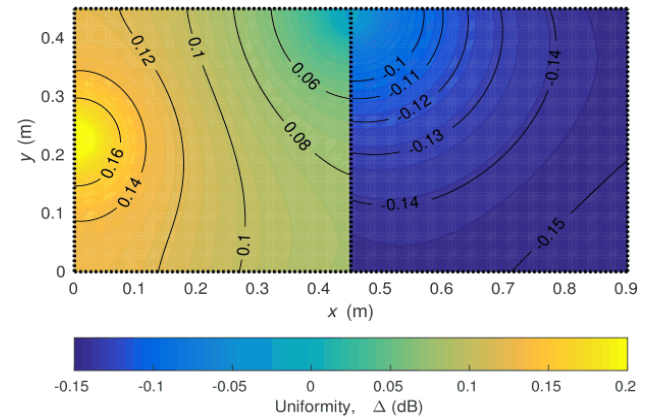


Figure 6. The diffuse energy density uniformity for Enclosure with partition and no absorbing cylinder.

5.2. Enclosure with partition

The partition divides the Enclosure into two equal size cavities, with a small coupling gap between them. Figure 6 compares the diffusion result with the PWB prediction when no absorbing cylinder is present. It can be seen that the two solutions agree within ~ 0.16 dB. As the absorption rate of the walls and aperture is small, little non-uniformity is present in the energy density of either cavity.

Figure 7 shows the case with an absorbing cylinder in the right half of the divided enclosure. Both cavities show an

increased non-uniformity in the energy density with a maximum of ~ 2.2 dB near the coupling gap in the right hand cavity.

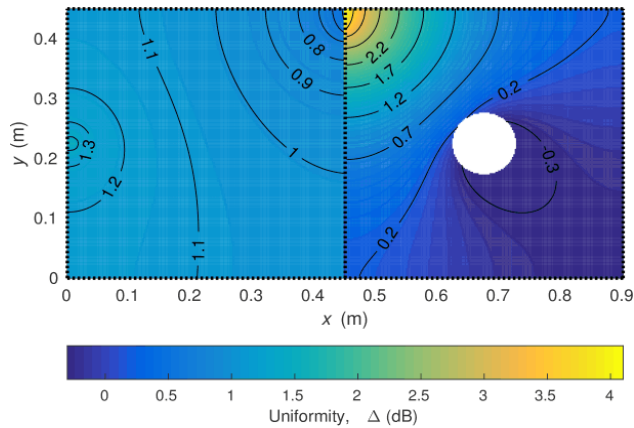


Figure 7. The diffuse energy density uniformity for enclosure with partition and an absorbing cylinder.

Figure 8 compares the results from the EDM, PWB and measurements using small probe antennas on the top of the enclosure along a number of lines in the x -direction. The agreement of EDM with the measurements here is not quite as good as in Figure 5.

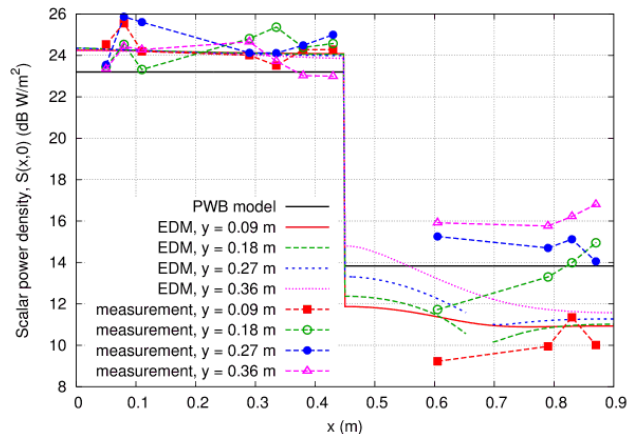


Figure 8. Comparing the PWB, diffusion and measured results along different lines in the $z = h$ plane of the enclosure with partition and absorbing cylinder at 8.5 GHz.

6. Conclusions

Diffusion-based modelling of reverberant environments requires a little greater computational resource than the power balance method but it provides useful information about the effect of significant absorbers on the field uniformity. The effort required is still substantially less than that required for a full wave solution. The 2-dimensional examples shown here were solved in seconds. A 3-dimensional full wave solution of a reverberant enclosure takes days of computer time.

7. References

1. P. Corona; G. Latmiral, E. Paolini, and L. Piccioli, "Use of a Reverberating Enclosure for Measurements of

Radiated Power in the Microwave Range", *IEEE Trans. Electromagn. Compat.*, no. 2, pp 54-59, May, 1976.

2. D. A. Hill, "Plane wave integral representation for fields in reverberation chambers", *IEEE Trans. Electromagn. Compat.*, vol. 40, no. 3, pp. 209-217, Aug. 1998.

3. D. A. Hill, M. T. Ma, A. R. Ondrejka, B. F. Riddle, M. L. Crawford and R. T. Johnk, "Aperture excitation of electrically large, lossy cavities", *IEEE Trans. Electromagn. Compat.*, vol. 36, no. 3, pp. 169-178, Aug. 1994.

4. I. Junqua, J.-P. Parmantier and F. Issac, "A network formulation of the power balance method for high-frequency coupling", *Electromagnetics*, vol. 25, no. 7-8, pp. 603-622, 2005.

5. J. Picaut, L. Simon and J.-D. Polack, "A mathematical model of diffuse sound field based on a diffusion equation", *Acta Acustica*, vol. 83, pp. 614-621, 1997.

6. I. D. Flintoft; A. C. Marvin, F. I. Funn, L. Dawson, X. Zhang, M. P. Robinson and J. F. Dawson, "Evaluation of the Diffusion Equation for Modelling Reverberant Electromagnetic Fields", *IEEE Trans. Electromagn. Compat.* vol.PP, no.99, pp.1-10, doi: 10.1109/TEMC.2016.2623356, 2017.

7. D. A. Hill, "Boundary Fields in Reverberation Chambers", *IEEE Trans. Electromagn. Compat.*, vol. 47, no. 2, 281-290, May, 2005.

8. F. Hecht, "New development in FreeFEM++", *Journal of Numerical Mathematics*, vol. 20, no. 3-4, pp. 251-265, 2012.

9. J. G. Kostas and B. Boverie, "Statistical model for a mode-stirred chamber", *IEEE Trans. Electromagn. Compat.*, vol. 33, no. 4, pp. 366-370, Nov. 1991.

10. X. Zhang, M. P. Robinson and I. D. Flintoft, "On measurement of reverberation chamber time constant and related curve fitting techniques", *2015 Joint IEEE Int. Symp. Electromagn. Compat. and EMC Europe*, Dresden, Germany, pp. 406-411, 16-22 Aug. 2015.